ELSEVIER

Physica B 273–274 (1999) 655–658

PHYSICA B

www.elsevier.com/locate/physb

Electron-paramagnetic-resonance studies of defects in electron-irradiated p-type 4H and 6H SiC

N.T. Son[a,*], P.N. Hai[a], P.T. Huy[b], T. Gregorkiewicz[b], C.A.J. Ammerlaan[b], J.L. Lindström[a,1], W.M. Chen[a], B. Monemar[a], E. Janzén[a]

[a]*Department of Physics and Measurement Technology, Linköping University, S-581 83 Linköping, Sweden*
[b]*Van der Waals-Zeeman Institute, University of Amsterdam, Valckenierstraat 65-67, NL-1018 XE Amsterdam, Netherlands*

Abstract

Defects in p-type 4H and 6H SiC irradiated by 2.5 MeV electrons were studied by electron paramagnetic resonance (EPR). Two anisotropic EPR spectra, labeled I and II, were observed in both 4H and 6H SiC. These spectra demonstrating triclinic symmetry of the center can be described by an effective electron spin $S = \frac{1}{2}$. The angle α between the direction of the principal g_z of the g-tensors and the c-axis is determined as 63° and 50° for spectra I and II, respectively. In the 6H polytype, a third also similar EPR spectrum was detected. Based on their similarity in the electronic structure (electron spin, symmetry, g values), annealing behavior and temperature dependence, these spectra are suggested to be related to the same defect occupying different inequivalent lattice sites in 4H and 6H SiC. A pair between a silicon vacancy and an interstitial is a possible model for the defect. © 1999 Elsevier Science B.V. All rights reserved.

Keywords: Silicon carbide; Defects; Electron paramagnetic resonance

1. Introduction

In a compound semiconductor such as SiC, vacancies, interstitials and also anti-site defects are created under high-energy-particle irradiation. The interaction between these primary defects leads to the formation of many possible complex centers. Although the vacancies in SiC seem to become mobile only at temperatures far above room temperature [1,2], different vacancy-associated complexes can already be formed without undergoing an anneal at higher temperatures [1]. An isolated defect such as a single vacancy will give rise to only one electron paramagnetic resonance (EPR) spectrum in the cubic lattice of the 3C SiC. In the 4H and 6H SiC, there are two and three inequivalent lattice sites, respectively, and hence a substitutional defect can give rise to two or three different spectra depending on its position. The one-to-one correspondence between the number of the spectra and the inequivalent lattice sites may also apply for vacancy-related complexes if the electron spins mainly locate in one of the constituents. A defect occupying different inequivalent lattice sites may give rise to different EPR spectra. This makes the defect study, which is already very complicated as experienced in electron-irradiated cubic semiconductors, more difficult in hexagonal SiC polytypes.

In the past, most of the EPR studies of intrinsic defects were reported for 3C and 6H SiC [1–5] and much less for the 4H polytype [6,7]. Recently, Cha and coworkers [8] have studied p-type 6H SiC irradiated with electrons and observed several low-symmetry EPR spectra (PC1, PC2 and PD), but no suggestion on defect identification has been made. In this work, we used EPR to study defects in p-type 4H and 6H SiC irradiated with 2.5 MeV electrons at room temperature. In 6H SiC, we also observed three anisotropic EPR spectra with an electron spin $S = \frac{1}{2}$,

---

[*] Corresponding author. Fax: + 46-13-142337.
E-mail address: son@ifm.liu.se (N.T. Son)

[1] Present address: Department of Solid State Physics, Lund University, Box 118, S-221 00 Lund, Sweden.

PII: S0921-4526(99)00597-9

which are very similar to those observed by Cha et al. [8]. Comparing the results in 6H and 4H SiC, it is suggested that all these EPR spectra are related to the same defect occupying different inequivalent lattice sites.

2. Experiment

Samples used in this work were p-type 4H and 6H SiC substrates from Cree Research Inc. The concentration of the Al acceptor is about 2.5×10^{18} cm^{-3} in 4H SiC and 4.4×10^{17} cm^{-3} in 6H SiC samples. These commercial substrates are off-axis wafers in which the plane's normal is not parallel to the c-axis but inclines an angle (~ 3.5° for 6H and ~ 8° for 4H polytypes) towards the [1 1 $\bar{2}$ 0] direction. The samples were irradiated by 2.5 MeV electrons with doses in the range 10^{16}–10^{17} cm^{-2} at room temperature. EPR measurements were performed on a K-band (~ 23 GHz), superheterodyne spectrometer, tuning to observe the dispersion of the susceptibility. During the experiments, the sample temperature can be regulated from 2.5 K to room temperature. For angular dependence studies of the EPR spectra the magnetic field was rotated in the (1 1 $\bar{2}$ 0) plane. Since the samples were cut from off-axis wafers, typical misalignments by an angle of about 3° and 8° for 6H and 4H SiC, respectively, were often present in the experiments. Due to this type of misalignment, the magnetic field was actually rotated in a plane, which inclined an angle φ with the (1 1 $\bar{2}$ 0) plane as illustrated in Fig. 1.

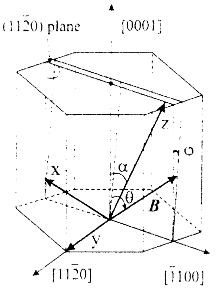

Fig. 1. Principal axes of the g-tensor and a typical sample misalignment occurring in the experiments. For off-axis samples, the magnetic field $\boldsymbol{B}$ was indeed rotating in a plane inclined an angle φ with the (1 1 $\bar{2}$ 0) plane.

3. Results and discussion

Several low-temperature EPR spectra were detected in p-type 4H and 6H SiC irradiated with electrons with a dose of 1×10^{17} cm^{-2}. Figs. 2(a) and 2(b) show the spectra in 4H and 6H SiC, respectively, recorded for the magnetic field $\boldsymbol{B}$ parallel to the c-axis. These spectra were not detected in as-grown materials. As can be seen in Fig. 2(a), three groups of lines with different intensities and line widths appear at around 825, 831 and 833 mT. The low-field lines in the region 823.5–826 mT as indicated by solid and dashed arrows in the figure belong to two different spectra, labeled I and II, respectively. The group of lines at around 831 mT belongs to unidentified defects. These lines severely overlap with each other at most directions of the magnetic field. The lines in the region 832–834 mT, labeled EI1 and EI2, belong to defects related to carbon and silicon vacancies [9], respectively. In the 6H polytype, similar groups of lines were also detected in the same region of the magnetic field [Fig. 2(b)] as in the case of 4H SiC. The low-field lines are also labeled I and II due to the similarity in the g-values and other aspects, which will be shown later. In addition to these, another more anisotropic spectrum was detected.

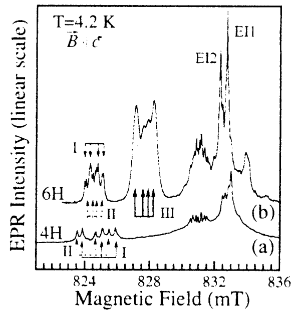

Fig. 2. EPR spectra observed in p-type (a) 4H and (b) 6H SiC irradiated with 2.5 MeV electrons with a dose of 1×10^{17} cm^{-2} for $\theta = 0$. The lines belong to spectra I, II and III are indicated by solid, dashed and thick solid arrows, respectively. Due to misalignment (Fig. 1), at this direction of $\boldsymbol{B}$ each spectrum should be observed as a group of three lines. In (b) the angle θ is not exactly zero so each spectrum appears as a group of four broader lines. The microwave frequencies are (a) $\nu = 23.335636$ and (b) $\nu = 23.332216$ GHz.

These lines, labeled III, are indicated by thick arrows in Fig. 2(b). The intensity of spectra I–III increases with increasing the dose of irradiation. However, when the dose reaches about 5×10^{17} cm^{-2}, these spectra disappear and another anisotropic spectrum, with an electron spin $S = 1$ is detected in both 4H and 6H SiC [10]. These EPR signals disappear at measurement temperatures above 25 K.

At some angles of the magnetic field, where the resonance lines are relatively strong and well separated, weak hyperfine structure lines can be seen. Fig. 3 shows, as an example, the hyperfine structure of the spectrum III in 6H SiC for the magnetic field $\boldsymbol{B}$ perpendicular to the c-axis. There are three satellites on each side of the main line (one of these is overlapping with other EPR lines of spectrum I). The total intensity of these satellites is about

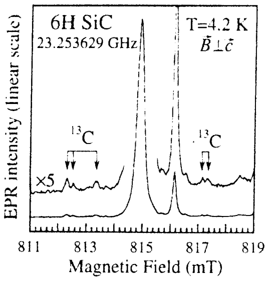

Fig. 3. Part of the EPR spectrum III in 6H SiC for$\boldsymbol{B}\,\|[\bar{1}\,1\,0\,0]$. The hyperfine structure due to the interaction with four ^{13}C atoms in the nearest-neighbor shell is indicated by arrows.

4.6% compared to that of the main line. This hyperfine structure is due to the interaction between the electron spin and the nuclear spins of the four ^{13}C atoms ($I = \frac{1}{2}$ and 1.1% natural abundance) in the nearest-neighbor shell. The hyperfine structure due to the interaction with ^{29}Si atoms ($I = \frac{1}{2}$ and 4.7% natural abundance) in the next-nearest-neighbor shell is not resolvable. This makes the line width of spectra I–III (typically ~ 0.3 mT) broader comparing to that of the carbon-vacancy-related EI1 center (~ 0.11 mT). Thus, the observation of the ^{13}C hyperfine structure indicates that the electron spin localizes at the silicon site in the lattice.

The experimental angular dependencies for spectra I and II in 4H SiC are shown in Fig. 4 by the open circles. As shown by the solid curves, each spectrum consists of three closed loops, which do not coincide at $\theta = 0$. This splitting is due to a sample misalignment off the c-axis as illustrated in Fig. 1. The fits to the experimental data were performed taking into account the sample misalignment and using the spin Hamiltonian

$$H = \mu_B \boldsymbol{B} \cdot \boldsymbol{g} \cdot \boldsymbol{S}, \qquad (1)$$

where the effective electron spin $S = \frac{1}{2}$ and μ_B is the Bohr magneton. The g-tensor is diagonalized in the principal coordinate system with g_z and g_x lying in the $(1\,1\,\bar{2}\,0)$ plane and g_y along the $[1\,1\,\bar{2}\,0]$ direction as depicted in Fig. 1. α is the angle between the principal z-axis and the c-axis of the crystal. The principal g-values and angles α deduced from the best fits for spectra I and II in 4H SiC are given in Table 1. A misorientation angle in this case was $\varphi = 9^\circ$. The simulated angular dependencies of spectra I and II using the obtained parameters and Eq. (1) are plotted in Fig. 4 as solid and dotted curves, respectively. The angular dependencies of the spectra in the 6H polytype are very similar to those in the 4H SiC. Least-squares fits to the experimental data using the spin Hamiltonian (1) with an effective electron spin $S = \frac{1}{2}$ were performed. The obtained g-values and corresponding angles α for spectra I–III are also given in Table 1.

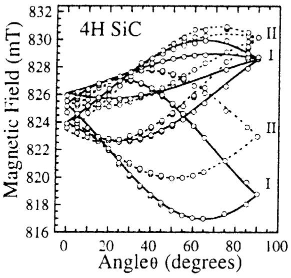

Fig. 4. Angular dependencies of spectra I and II in 4H SiC. The open circles represent the experimental data. The solid and dashed curves represent the simulated angular dependencies for spectra I and II, respectively, using the obtained parameters taking into account a misalignment angle $\varphi = 9^\circ$. The microwave frequency is $\nu = 23.335788$ GHz. The zero degree corresponds to the direction closest to the c-axis in the rotation plane, see Fig. 1. The angle of 90°, on the other hand, corresponds exactly to $\boldsymbol{B}\,\|[\bar{1}\,1\,0\,0]$.

Table 1
The principal g-values of spectra I–III in 4H and 6H SiC. α is the angle between the principal z and the c-axis. The error in the g-values is about $\pm$ 0.0003

Spectrum	Polytype	g_x	g_y	g_z	α (deg)
I	4H	2.0162	2.0035	2.0412	63 ± 0.5
	6H	2.0161	2.0061	2.0407	63 ± 0.5
II	4H	2.0144	2.0029	2.0337	50 ± 0.5
	6H	2.0139	2.0048	2.0323	50 ± 0.5
III	6H	2.0075	2.0021	2.0452	65.7 ± 0.5

The symmetry of spectra I–III is low (C_1). This suggests that the associated defects are not isolated impurities. Substitutional impurities in hexagonal SiC polytypes often have trigonal symmetry (C_{3v}) or, in the cases of off-center defects such as the shallow boron [11], both trigonal and monoclinic (C_{1h}) symmetries corresponding to the defect occupying the hexagonal and cubic sites, respectively. The symmetry axes in those cases usually coincide with the directions of the Si–C bonds, i.e. are either parallel to the c-axis or make an angle of about 71° with it. The same may apply for the cases of substitutional impurity–vacancy pairs. In our case, the spectra were only observed after irradiation and their intensities increase with increasing the dose of irradiation. This also indicates that they are related to intrinsic defects. The low symmetry in this case also rules out the possibility of an anti-site defect, which should have the same symmetry as the substitutional impurities. Together with the hyperfine structure described above, it can be concluded that the silicon vacancy is involved in the defects.

Experimental data [2,6] and a recent calculation [12] showed that the silicon vacancy in the hexagonal polytypes is undistorted or has axial (C_{3v}) symmetry depending on its charge states. According to this calculation [12], the geometrical changes around a silicon vacancy in the case of the positive charge state ($S = \frac{1}{2}$) will lead to the axial symmetry for the silicon vacancy at both cubic and hexagonal sites. Since its ground state lies close to the maximum of the valence band [12], the center would be observable in p-type material over a wide temperature range. These do not agree with our observation. Spectra I–III have a lower symmetry (C_1) and can be detected in a very narrow temperature range. Therefore, these spectra are attributed to complex centers involving a silicon vacancy.

Under high-energy electron bombardment, vacancies and interstitials are created. In SiC, vacancies are stable at room temperature [1,2]. A part of the interstitials may be recaptured by nearby vacancies–leading to either the restoration of the lattice from damages or the creation of antisites. In addition to these dominant isolated defects, other types of complex centers such as divacancies or vacancy–interstitial pairs may be possible. Coupling between the vacancies often leads to the formation of vacancy pairs with the electron spin $S = 1$ and specific directions of the defect axis as detected in 6H SiC [4]. Their formation may be enhanced under annealing at elevated temperatures when the vacancies become mobile. In the samples irradiated at ~ 400°C, these spectra were not detected, but instead a carbon vacancy pair was observed. The electron spin, the symmetry and the formation conditions of the studied centers are clearly different from that of the divacancies. In both polytypes, spectra I–III were found to be partially quenched after keeping the samples at room temperature for a few weeks. These signals gradually decrease with increasing the annealing temperature and disappear at around 700°C, which is close to the anneal-out temperature of the silicon vacancy [1]. A complex center involving a vacancy and an interstitial (or an impurity at interstitial positions) is a possible model for these centers. In this case, the electron spin may be localized mainly at the silicon vacancy but not at the interstitial. The defect is then site sensitive as a substitutional center and may give rise to different spectra corresponding to different inequivalent lattice sites.

In 4H and 6H SiC samples irradiated with different doses, spectra I–III always appear together with similar intensity ratios and line shapes. A similarity in temperature dependence and annealing behavior is also observed for these spectra. As can be seen from Table 1, the principal g-values of these spectra in both polytypes are very similar. Therefore, it is suggested that these spectra belong to the same defect. Spectra I and II may correspond to the defect occupying the quasi-cubic and hexagonal sites, respectively. Spectrum III then corresponds to the defect at the other cubic site of the 6H SiC lattice.

In summary, we have observed two and three EPR spectra in electron-irradiated, p-type 4H and 6H SiC, respectively. All the spectra have the same symmetry (C_1) and an effective electron spin $S = \frac{1}{2}$. A paired center between a silicon vacancy and an interstitial (or an impurity at an interstitial position) is a possible model of the defects. Based on the similarity in the electronic structure, annealing behavior, temperature dependence and formation conditions, these spectra are suggested to belong to the same defect, which occupies different inequivalent lattice sites in 4H and 6H SiC.

Acknowledgements

Support for this work was provided by the Swedish Research Council for Engineering Sciences (TFR), the Swedish Natural Science Research Council (NFR), the SSF program SiCEP and ABB Corporate Research.

References

[1] H. Itoh, A. Kawasuso, T. Ohshima, M. Yoshikawa, I. Nashiyama, S. Tanigawa, S. Misawa, H. Okumura, S. Yoshida, Phys. Stat. Sol. A 162, (1997) 173, and reference therein.

[2] J. Schneider, K. Maier, Physica B 185 (1993) 199.

[3] L.A. de S. Balona, J.H.N. Loubser, J. Phys. C 3 (1970) 2344.

[4] V.S. Vainer, V.A. Ilin, Sov. Phys. Solid State 23 (1981) 2126.

[5] E. Sörman, N.T. Son, W.M. Chen, O. Lindström, J.L. Kordina, E. Janzén, in: The Physics of Semiconductors, World Scientific, Singapore, 1996, p. 2649.

[6] T. Wimbauer, D. Volm, B.K. Meyer, A. Hofstaetter, A. Scharmann, in: The Physics of Semiconductors, World Scientific, Singapore, 1996, p. 2645.

[7] E. Sörman, N.T. Son, W.M. Chen, C. Hallin, J.L. Lindström, E. Janzén, Mater. Sci. Forum 258 (1997) 685.

[8] D. Cha, H. Itoh, N. Morishita, A. Kawasuso, T. Ohshima, Y. Watanabe, J. Ko, K. Lee, I. Nashiyama, Mater. Sci. Forum 264 (1998) 615.

[9] N.T. Son, W.M. Chen, J.L. Lindström, B. Monemar, E. Janzén, Mater. Sci. Eng. B. 61–62 (1999) 202.

[10] N.T. Son, W.M. Chen, J.L. Lindström, B. Monemar, E. Janzén, Phys. Scripta T 79 (1999) 46.

[11] T. Matsumoto, O.G. Poluektov, J. Schmidt, E.N. Mokhov, P.G. Baranov, Phys. Rev. B 55 (1997) 2219.

[12] A. Zywietz, J. Furthmüller, F. Bechstedt, Phys. Rev. B 59 (1999) 15166.